High Energy Neutrino Astronomy: The Experimental Road

Christian Spiering [a]

[a]DESY Zeuthen, Platanenallee 6, D-15738 Zeuthen, Germany

The next ten years promise to be a particularly exciting decade for high energy neutrino astrophysics. The frontier of TeV and PeV energies is presently being tackled by large, expandable arrays constructed in open water or ice. Detectors tailored to record acoustic, radio, fluorescence or air shower signatures from neutrino interactions at PeV – EeV energy are being designed in parallel. During the next decade, the sensitivity to neutrinos from TeV to EeV energies may improve by 2 to 3 orders of magnitude. This talk reviews methods, status and prospects of detectors and sketches a scenario for the experimental progress.

1. Introduction

Whereas MeV neutrino astronomy has been established by the observation of solar neutrinos and neutrinos from supernova SN1987, neutrinos with energies of GeV to PeV which must accompany the production of high energy cosmic rays still await discovery. Detectors underground have turned out to be too small to detect the feeble fluxes of energetic neutrinos from cosmic accelerators. The high energy frontier of TeV and PeV energy is currently being tackled by much larger, expandable arrays constructed in open water or ice. Detectors tailored to record acoustic, radio, fluorescence or air shower signatures from neutrino interactions at EeV energy (= 10^9 GeV) and above are being designed in parallel [1]. Fig. 1 sketches the energy domains of different techniques.

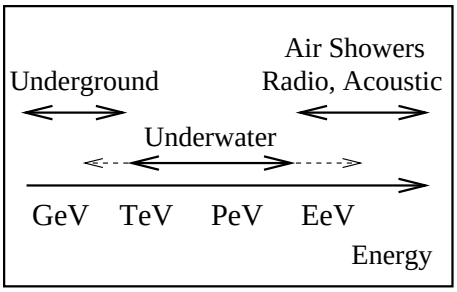

Figure 1. Energy range of the various detection techniques (see below). Optical Cherenkov detectors, although optimized to the TeV-PeV range, are sensitive also at lower and higher energies, as indicated by the dashed lines.

2. Physics Goals

The central goal of high energy neutrino telescopes is to settle the origin of high energy cosmic rays [2,3]. The directional information of these charged particles - protons, light and heavy nuclei - is lost due to deflection in cosmic magnetic fields (apart from the extreme energies above 10^{10} GeV where deflection is negligible). Source tracing, i.e. *astronomy*, is only possible by neutral, stable particles like γ rays and neutrinos. In contrast to γ rays which may come from pure electron acceleration, only neutrinos provide incontrovertible evidence of proton acceleration. On top of that, neutrinos do not suffer from absorption by the omnipresent infrared or radio background when propagating through space. The range of TeV γ rays is only about 100 Mpc, at PeV even only 10 kpc, i.e. about the radius of our Galaxy. Therefore, the topology of the far distant high energy Universe may possibly be investigated only with neutrinos.

The physics goals of high energy neutrino telescopes include:

a) Search for neutrinos from cosmic acceleration processes in galactic sources like micro quasars or supernova remnants (SNR), or extragalactic sources like active galactic nuclei (AGN) or gamma ray bursts (GRB),

b) search for ultra-high energy (UHE) neutrinos from interactions of UHE cosmic rays with the photons of cosmic 3K microwave background (the so called GZK neutrinos [4]), from topological defects (TD) or from the decay of super-heavy particles,

c) search for neutrinos from the annihilation of Weakly Interacting Massive Particles (WIMPs),

d) search for magnetic monopoles,

e) monitoring our Galaxy for MeV neutrinos from supernova bursts.

Most models related to sources of type *a)* assume acceleration by shock waves propagating in accretion discs around black holes or along the extended jets emitted perpendicularly to the disk (bottom-up models). Neutrinos are generated in decays of mesons produced by interactions of the accelerated charged particles with ambient matter or with photon gas.

$$p + p(\gamma) \rightarrow p(n) + \pi$$
$$\searrow \mu + \nu$$

The neutrino energy spectrum of many models follows an E_ν^{-2} behaviour, at least over a certain range of energy. Assuming an E_ν^{-2} form and normalizing the neutrino flux to the measured flux of cosmic rays at highest energies leads to an upper bound of $dN/dE_\nu \sim 5 \times 10^{-8} E_\nu^{-2}$ GeV^{-1} cm^{-2} s^{-1} sr^{-1} to the diffuse neutrino flux (i.e. the flux integrated over all possible sources) [5]. Reasonably weakened assumptions loosen this bound by more than one order of magnitude to $10^{-6} E_\nu^{-2}$ GeV^{-1} cm^{-2} s^{-1} sr^{-1} [6,7](see also Fig.14). The so-called top-bottom scenarios of type *b)* are suggestive for the explanation of highest energy cosmic rays. In this scenario, high energy particles would be "born" with high energies, and not accelerated from low to high energies, as in the standard bottom-up scenarios.

We will focus to *a)* and *b)* in the following and refer to [2,8,9,10] and references therein for more information on *c)* - *e)*.

3. Cherenkov telescopes under water and ice

Optical underwater/ice neutrino detectors consist of a lattice of photomultipliers (PMs) housed in transparent pressure spheres which are spread over a large open volume in the ocean, in lakes or in ice. In most designs the spheres are attached to strings which - in the case of water detectors - are moored at the ground and held vertically by buoys. The typical spacing along a string is 10-20 meters, and between strings 30-100 meters. The spacing is incomparably large compared to Super-Kamiokande. This allows to cover large volumes but makes the detector practically blind with respect to phenomena below 10 GeV.

The PMs record arrival time and amplitude of Cherenkov light emitted by muons or particle cascades. The accuracy in time is a few nanoseconds. Fig. 2 sketches the two basic detection modes.

In the *muon* mode, high energy neutrinos are inferred from the Cherenkov cone accompanying muons which enter the detector from below. Such upward moving muons can have been produced only in interactions of muon neutrinos having crossed the earth. The effective volume considerably exceeds the actual detector volume due to the large range of muons (about 1 km at 300 GeV and 24 km at 1 PeV). Muons which have been generated in the earth atmosphere above the detector and punch through the water or ice down to the detector, outnumber neutrino-induced upward moving muons by several orders of magnitude and have to be removed by careful up/down assignment. At energies above a few hundred TeV, where the earth is going to become opaque even to neutrinos, muons arrive only from directions close to the horizon, at EeV energies even only from the upper hemisphere. Most of these muons can be distinguished from down going atmospheric muons due to their higher energy deposition.

Apart from elongated tracks, *cascades* can be detected. Their length increases only like the logarithm of the cascade energy. With typically 5-10 meters length, and a diameter of the order of 10 cm, cascades may be considered as quasi point-like compared to the spacing of photomultipliers

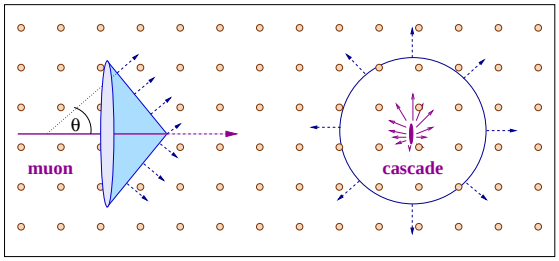

Figure 2. Detection of muon tracks (left) and cascades (right) in underwater detectors.

in Cherenkov telescopes. The effective volume for cascade detection is close to the geometrical volume. While for present telescopes it therefore is much smaller than that for muon detection, for kilometer-scale detectors and not too large energies it can reach the same order of magnitude like the latter.

Underwater/ice telescopes are optimized for the detection of muon tracks and for energies of a TeV or above, by the following reasons:

a) The flux of neutrinos from cosmic accelerators is expected to be harder than that of atmospheric neutrinos above 1 TeV, yielding a better signal-to-background ratio at higher energies.

b) Neutrino cross section and muon range increase with energy. The larger the muon range, the larger is the effective detection volume.

c) The mean angle between muon and neutrino decreases with energy like $E^{-0.5}$, with a pointing accuracy of about one degree at 1 TeV.

d) Mainly due to pair production and bremsstrahlung, the energy loss of muons increases with energy. Above 1 TeV, this allows to estimate the muon energy from the larger light emission along the track.

The development in this field was stimulated by the **DUMAND** project close to Hawaii which was cancelled in 1995. The breakthrough came from the other pioneering experiment located at a depth of 1100 m in the Siberian Lake Baikal. The **Baikal** collaboration not only was the first to deploy three strings (as necessary for full spatial reconstruction [11]), but also reported the first atmospheric neutrinos detected underwater ([12], see Fig. 4, left). At present, NT-200 is taking data, an array comprising 192 mushroom shaped 15"-PMs at eight strings. A moderate upgrade (NT200+) is planned for 2003/04 (see fig.3, which shows at the top the small, compact NT-200 array plus three sparsely instrumented distant strings forming together NT200+). NT200+ will allow a significantly improved cascade reconstruction within the volume framed by the new strings.

With respect to its size, NT-200 has been surpassed by the **AMANDA** detector [13]. Rather than water, AMANDA uses the 3 km thick ice layer at the geographical South Pole. Holes are drilled with hot water, and strings with PMs are frozen into the ice. With 677 PMs at 19 strings, most at depths between 1500-2000 m, the present AMANDA-II array reaches an area of a few 10^4 m^2 for 1 TeV muons. Although still far below the square kilometer size suggested by most theoretical models, AMANDA-II may be the first detector with a realistic discovery potential with respect to extraterrestrial high energy neutrinos. Limits obtained from the analysis of data taken with the smaller ten-string detector AMANDA-B10 in 1997 are similar to or below those limits which have been obtained by underground detectors over more than a decade of data taking. The limit on the diffuse flux from unresolved sources with an assumed E^{-2} spectrum is $0.8 \cdot 10^{-6} E_\nu^{-2}$ GeV^{-1} cm^{-2} s^{-1} sr^{-1} [14], below loosest theoretical bounds [6,7], slightly below the corresponding Baikal limit and nearly an order of magnitude below limits from underground experiments. AMANDA limits on point sources on the Northern sky [15] complement the limits obtained from detectors on the Northern hemisphere for the Southern sky (see Fig. 15). The sensitivity of AMANDA-B10 has been verified by samples of events which are dominated by atmospheric neutrinos [16]. Fig. 4 (right) shows a neutrino event taken with AMANDA-B10, Fig. 5 the sky map of first neutrino candidates taken in 1997.

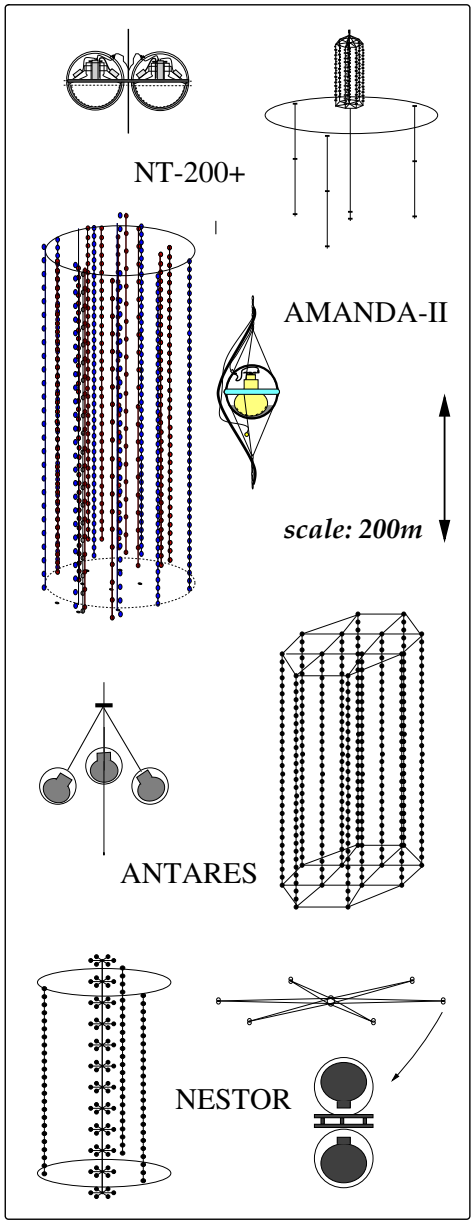

Figure 3. BAIKAL, AMANDA, ANTARES and NESTOR. Detectors are shown on the same scale. BAIKAL is shown in its planned 2004 configuration NT200+, ANTARES with its 12-string configuration planned for 2005 and NESTOR with an envisaged "ring" made of old DUMAND modules. For AMANDA, modules shallower than 1.5 km and deeper than 2.0 km are omitted in this figure.

Based on the experience from AMANDA, a cubic kilometer detector, **ICECUBE** [18], is going to be deployed at the South Pole. It will consist of 4800 PMs at 80 vertical strings, with 125 m inter-string-distances and a 16 m spacing between the PMs along a string (see fig.6). The 8-inch AMANDA PMs will be replaced by 10-inch PMs. As for the recently upgraded Amanda read-out, full transient waveforms will be recorded from every PM.

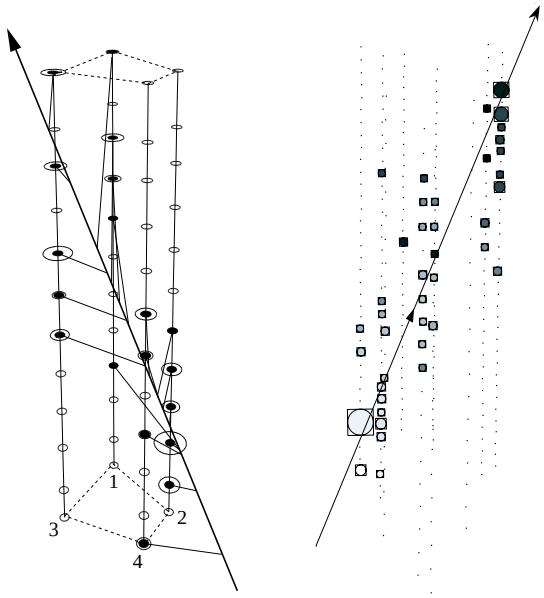

Figure 4. Left: one of the first clearly upward moving muons recorded with the 1996 four-string-stage of the Baikal detector. Small ellipses denote PMs. Hit PMs are black, with the size of the disc proportional to the recorded amplitude. The arrow line represents the reconstructed muon track, the thin lines the photon pathes. Right: Upward muon recorded by the 1997 version of AMANDA. Small dots denote the PMs arranged at ten strings. Hit PMs are highlighted by boxes, with the degree of shadowing indicating the time (dark being late), and the size of the symbols the measured amplitude. Note the different scales: the height of the Baikal array is 72 meters, that of AMANDA nearly 500 meters.

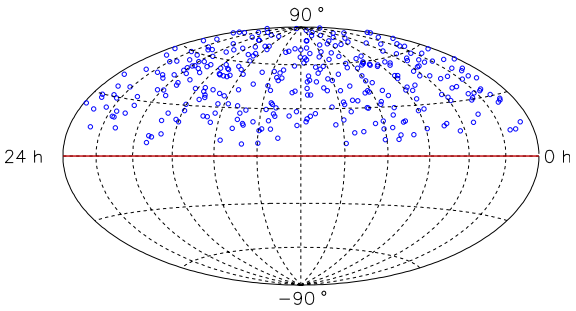

Figure 5. Sky map of 300 neutrino candidates taken with AMANDA B10 in 1997. No indication of extraterrestrial point sources on top of atmospheric neutrinos are found.

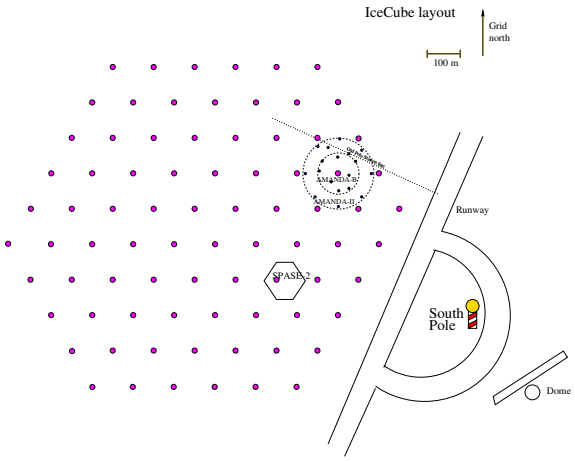

Figure 6. Top view of the IceCube detector

Two projects for large neutrino telescopes are under construction in the Mediterranean - **ANTARES** [19] and **NESTOR** [20] - see fig.3. Both have assessed the relevant physical and optical parameters of their sites, developed deployment methods, performed a series of operations with a few PMs and layed underwater cables to the future locations of the detectors. ANTARES and NESTOR envision different deployment schemes and array designs. The NESTOR group plans to deploy a tower of several floors, each carrying 12 PMs at 16 m long arms. Later, a ring consisting of 72 former DUMAND PMs is planned. The ANTARES detector will consist of 12 strings, each equipped with 30 triplets of PMTs. This detector will have an area of about $2 \cdot 10^4$ m^2 for 1 TeV muons - similar to AMANDA-II - and is planned to be fully deployed by the end of 2004. In addition to these two advanced projects, there is an Italian initiative, **NEMO**, which finished site investigations at a location 80 km from Sicily and is now in the phase of prototype studies for a cubic kilometer detector [21]. At the same time, also ANTARES, BAIKAL and NESTOR envisage larger arrays, possibly of cubic kilometer size.

There have been longstanding discussions about the best location for a future large neutrino telescope. What concerns geographic location, one detector on each hemisphere are necessary for full sky coverage. With respect to optical properties, water detectors in oceans seem to be favoured: although the absorption length of Antarctic ice at Amanda depths is nearly twice as long as in oceans (and about four times that of Baikal), ice is characterized by strong light scattering, and its optical parameters vary with depth. Light scattering leads to a considerable delay of Cherenkov photons. On the other hand ice does not suffer from the high potassium content of ocean water or from bioluminescence. These external light sources result in counting rates ranging from several tens of kHz to a few hundred kHz, compared to less than 500 Hz pure PM dark count rate in ice. Depth arguments favour oceans. The seabed at the NESTOR site is deepest (4 km), closely followed by NEMO (3.5 km). With only 2.5 km, the ANTARES ground is at about the same depth as the lowest AMANDA modules. Note, however, that the depth argument lost some of its initial strength after BAIKAL and AMANDA had developed reconstruction methods which effectively reject even the high background at shallow depths. Actually, the main advantage of great depths is the possibility to look higher above horizon, i.e. an

increased angular acceptance. For water, a detector at greater depth suffers less from sedimentation of biomatter and from increased noise rates due to bio-luminescence. What counts most, at the end, are basic technical questions like deployment, or the reliability of the single components as well as of the whole system. Systems with a non-hierarchical structure like AMANDA (where each PM has its own 2 km cable to surface) will suffer less from single point failures than water detectors do. In the case of water, longer distances between detector and shore station have to be bridged. Consequently, not every PM can get its own cable to shore, resulting in a hierarchical system architecture. This drawback of water detectors may be balanced by the fact that they allow retrieval and replacements of failed components, as the BAIKAL group has demonstrated over many years.

Most likely, the present efforts will converge to two cubic kilometer detectors for very high energy neutrinos, ICECUBE at the South Pole and one in the Mediterranean.

4. Acoustic detection

Acoustic particle detection was proposed first in the fifties [22] and experimentally proven two decades later [23]. A high energy particle cascade deposits energy into the medium via ionization losses, which is immediately converted into heat. The effect is a fast expansion, generating a bipolar acoustic pulse with a width of a few ten microseconds in water or ice (see fig.7). Transverse to the pencil-like cascade (diameter about 10 cm) the radiation propagates within a disk of about 10 m thickness (the length of the cascade) into the medium. The signal power peaks at 20 kHz where the attenuation length of sea water is a few kilometers, compared to a few tens of meters for light. Given a large initial signal, huge detection volumes can be achieved. Provided efficient noise rejection, acoustic detection might be competitive with optical detection at multi-PeV energies [24,25].

Present initiatives (see [10]) envisage combinations of acoustic arrays with optical Cherenkov detectors (NESTOR, ANTARES, ICECUBE) or the use of existing sonar arrays for submarine detection close to Kamchatka and in the Black Sea [26]. Most advanced is **AUTEC**, a project using a very large hydrophone array of the US Navy, close to the Bahamas [27]. The existing array of 52 hydrophones spans an area of 250 km^2 and has good sensitivity between 1-50 kHz. It is expected to trigger on events above 100 EeV with a tolerable false alarm rate.

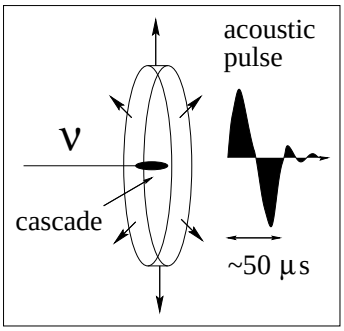

Figure 7. Acoustic emission of a particle cascade

5. Radio detection

Electromagnetic showers generated by high energy electron neutrino interactions emit coherent Cherenkov radiation. Radio Cherenkov emission was predicted in 1962 [28] and confirmed by recent measurements at SLAC and ANL [29]. Electrons are swept into the developing shower, which acquires a negative net charge from the added shell electrons . This charge propagates like a relativistic pancake of 1 cm thickness and 10 cm diameter. Each particle emits Cherenkov radiation, with the total signal being the resultant of the overlapping Cherenkov cones. For wavelengths larger than the cascade diameter, coherence is observed and the signal rises proportional to E^2, making the method attractive for high energy cascades. The bipolar radio pulse has a width of 1-2 ns. In ice as well as in salt domes, attenuation lengths of several kilometers can be obtained, depending on the frequency band, the temperature of the ice, and the salt quality. Thus, for energies above a few tens of PeV, radio detec-

tion in ice or salt might be competitive or superior to optical detection [25].

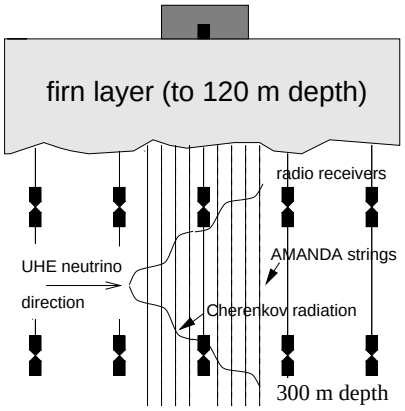

Figure 8. The RICE detector at South Pole

A prototype Cherenkov radio detector called **RICE** is operating at the geographical South Pole [30]. Twenty receivers and emitters are buried at depths between 120 and 300 m (fig.8). From the non-observation of very large pulses, a limit of about $10^{-4}E_\nu^{-2}$ GeV^{-1} cm^{-2} s^{-1} sr^{-1} has been derived for energies above 100 PeV.

SALSA, a R&D project study for radio detection in natural salt domes, promises to get a limit about three orders of magnitude better [31]. **ANITA** (ANtarctic Impulsive Transient Array) is an array of radio antennas planned to be flown at a balloon on an Antarctic circumpolar path in 2006 [32]. From 35 km altitude it may record the radio pulses from neutrino interactions in the thick ice cover and monitor a really huge volume (see fig.9). The expected sensitivity from a 30 day flight is about $10^{-7}E_\nu^{-2}$ GeV^{-1} cm^{-2} s^{-1} sr^{-1} at 10 EeV.

Most exotic is the Goldstone Lunar Ultrahigh Energy Neutrino Experiment, **GLUE** (see fig.10). It has searched for radio emission from extremely-high energy cascades induced by neutrinos or cosmic rays skimming the moon surface [33]. Using two NASA antennas, an upper limit of $10^{-4}E_\nu^{-2}$ GeV^{-1} cm^{-2} s^{-1} sr^{-1} at 100 EeV has been obtained.

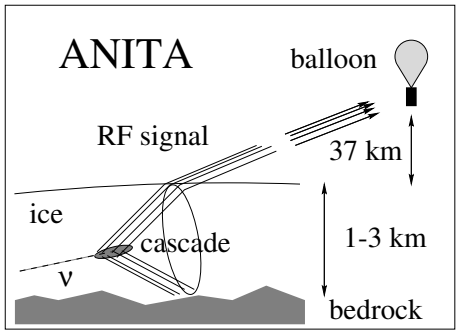

Figure 9. The ANITA balloon project

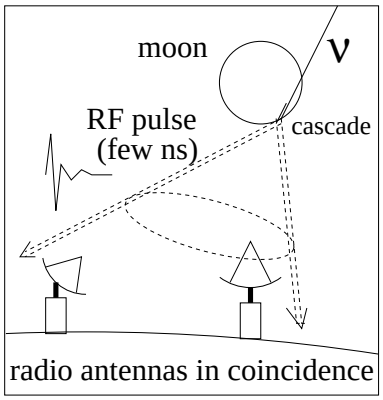

Figure 10. The Goldstone Lunar Ultrahigh Energy neutrino Experiment GLUE.

6. Detection of neutrino energies via air showers

At supra-EeV energies, large extensive air shower arrays like the **AUGER** detector in Argentina [34] or the telescope array [35] may seek for horizontal air showers due to neutrino interactions deep in the atmosphere (showers induced by charged cosmic rays start on top of the atmosphere). Figure 11 explains the principle. AUGER consists of an array of water tanks going to span an area of more than 3000 km^2 and will record the Cherenkov light of air-shower particles crossing the tanks. It is combined with telescopes looking for the atmospheric fluorescence

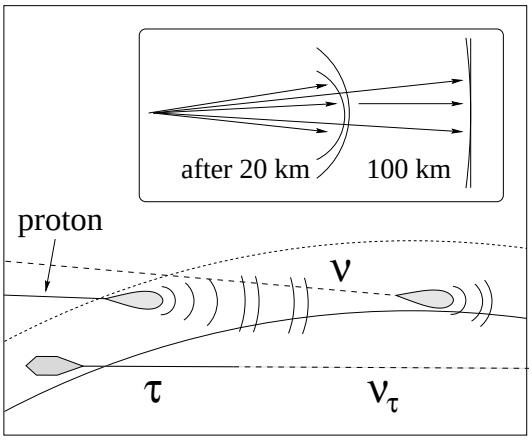

Figure 11. Detection of fluorescence light emitted by horizontal or upward directed air showers from neutrino interactions.

light from air showers. The optimum sensitivity window for this method is at 1-100 EeV, the effective detector mass is between 1 and 20 Giga-tons, and the estimated sensitivity is of the order of $10^{-8} E_\nu^{-2}$ GeV^{-1} cm^{-2} s^{-1} sr^{-1}. An even better sensitivity might be obtained for tau neutrinos, ν_τ, scratching the Earth and interacting close to the array. The charged τ lepton produced in the interaction can escape the rock around the array, in contrast to electrons, and in contrast to muons it decays after a short path into hadrons. If this decay happens above the array or in the field of view of the fluorescence telescopes, the decay cascade can be recorded. Provided the experimental pattern allows clear identification, the acceptance for this kind of signals can be large. For the optimal energy scale of 1 EeV, the sensitivity might reach $10^{-8} E_\nu^{-2}$ GeV^{-1} cm^{-2} s^{-1} sr^{-1}. A variation of this idea is to search for tau lepton cascades which are produced by horizontal PeV neutrinos hitting a mountain and then decay in a valley between target mountain and an "observer" mountain – see fig.12 [36].

Already eight years ago, the **Fly's Eye** collaboration [37], and more recently, the Japanese **AGASA** collaboration [38] have practiced the search mode of horizontal air showers. AGASA

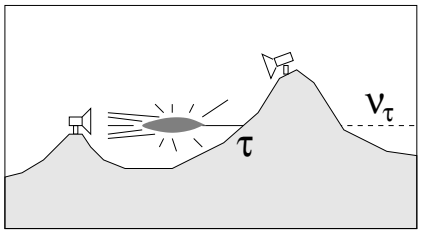

Figure 12. Detection of tau neutrino showers behind a mountain.

derived an upper limit of the order of 10^{-5} in the units given above - only just one order of magnitude above some predictions for AGN jets and for topological defects.

Heading to higher energies leads to space based detectors monitoring larger volumes than visible from any point on the Earth surface. The projects **EUSO** [39] and **OWL** [40] foresee to launch large mirrors with optical detectors to 500 km height. The mirrors would look down upon the atmosphere and search for nitrogen fluorescence signals due to neutrino interactions (see fig.13). The monitored mass would be up to 10 Tera-tons, with an energy threshold of about 10^{10} GeV.

Finally, I mention the idea to detect the radio emission from cosmic ray and neutrino induced air showers with low frequency radio telescopes, as dicussed in [41].

7. Scenario for the next decade

The next ten years promise to be a particularly exciting decade for high energy neutrino astrophysics. Figures 14 and 15 sketch possible scenarios to move the frontier towards unprecedented sensitivities.

Like every estimate of time scales and expected physics performance, this scenario should be taken with caution. Notorious time delays in the realization of projects on the one hand, and possible new approaches on the other, will likely modify the evolution. In addition, new techniques have to be fully understood – their sensitivity to signals as well as the backgrounds! With AMANDA and BAIKAL, the optical un-

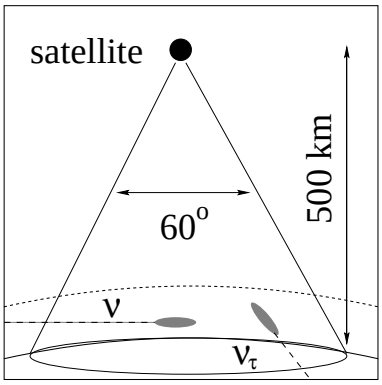

Figure 13. Principle of neutrino detection by satellite experiments.

derwater/ice technique has mastered this phase: downgoing muons and atmospheric neutrinos provided an invaluable calibration source. The energy range of acoustic or radio techniques as described in sections 4 and 5, however, is beyond the range covered by atmospheric neutrinos or normal cosmic rays. Calibration of the detectors in the absence of a surefire signal will be a challenge.

Figure 14 addresses the sensitivity to diffuse fluxes, i.e. integrating over the full angular acceptance of the detectors. The scale is set by the known flux of atmospheric neutrinos, by the bounds derived from observed fluxes of charged cosmic rays (W&B [5] and, with less stringent assumptions, the lower MPR curve [7]), by gamma rays (horizontal MPR line which assumes that cosmic rays are mostly confined in the cosmic source region and only gammas and neutrinos escape), and by specific model predictions [42]. The figure shows two of the latter, one for the predicted flux of GZK neutrinos at ultra-high energies (see item *b)* above), the other for a model on neutrinos from Active Galactic Nuclei, peaking at TeV-PeV energies (Stecker and Salomon, SS [43]). The majority of the limits shown are published as "differential" limits, defining the flux sensitivity as the neutrino flux which gives at least one observed event per decade of energy per year (assuming negligible background). The limits published for AMANDA assume an E^{-2} flux. They come from two separate analyses, the one studying upward muons tracks [44], the other downward tracks of very high energy which are unlikely being due to muons generated in the atmosphere [45]. Both analyses, however, properly account for the background of these atmospheric muons. The lines marked *1* and *2* extend over the energy range containing 90% of the events expected from an E^{-2} flux. For better illustration of the progress in time and over all the energy range, the AMANDA limits as well as the limits expected for ICECUBE have been translated to limits differentially per energy decade.

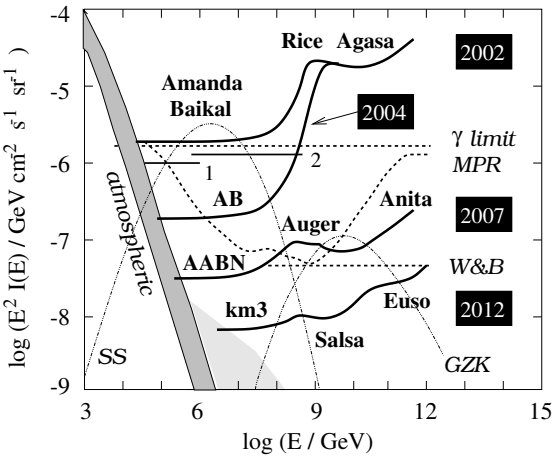

Figure 14. Scenario for the improvement of experimental sensitivities to diffuse extraterrestrial fluxes of high energy neutrinos. AB = Amanda, Baikal, AABN = Amanda, Antares, Baikal, Nestor. *1,2,:* Amanda limits obtained from the analysis of upward (1) and high energy downward (2) tracks, assuming an E^{-2} spectrum. The grey band denotes the flux of atmospheric neutrinos, with the excess at high energies being an estimate for the contribution from prompt muons and neutrinos due to charm decays in air showers. Dashed lines indicate various theoretical bounds, the 2 thin curves specific flux predictions (see text).

The present frontier is defined by TeV-PeV limits obtained by AMANDA and BAIKAL, and by PeV-EeV limits from the South Pole radio array RICE and the Japanese AGASA air shower array. Note that the Baikal/Amanda limits just reached a level sufficient to test (and actually to exclude) the model shown. The progress over the next 2 years will come from AMANDA and BAIKAL. After that, the Mediterranean telescopes – ANTARES and NESTOR – will start to contribute, flanked by AUGER and the ANITA balloon mission at high energies. This could result in an improvement of about two orders of magnitude over the full relevant energy range. Actually, five years from now a large variety of models might have been tested, including several predictions for neutrinos at GZK energies [42]. Finally, in ten years from now, the TeV-PeV sensitivity will be defined by the cubic kilometer arrays at the South Pole and in the Mediterranean (marked as "km3"). At the high energy frontier, a SALSA-like experiment, and still higher, satellite detectors, might push the limit down by about three orders of magnitude compared to 2002.

Most likely, the first signal with clear signature will be a point source, possibly a transient signal which is easiest to identify. Figure 15 sketches a possible road until 2012. Best present limits are from MACRO, Super-Kamiokande (Southern sky) and AMANDA-B10 (Northern sky). This picture will not change until the Mediterranean detectors come into operation. AMANDA and ANTARES/NESTOR have the first realistic chance to discover an extraterrestrial neutrino source. The ultimate sensitivity for the TeV-PeV range is likely reached by the cubic kilometer arrays. This scale is set by many model predictions for neutrinos from cosmic accelerators or from dark matter decay. However, irrespective of any specific model prediction, these gigantic detectors, hundred times larger than AMANDA and thousand times larger than underground detectors, will hopefully keep the promise for any detector opening a new window to the Universe: to detect *unexpected* phenomena.

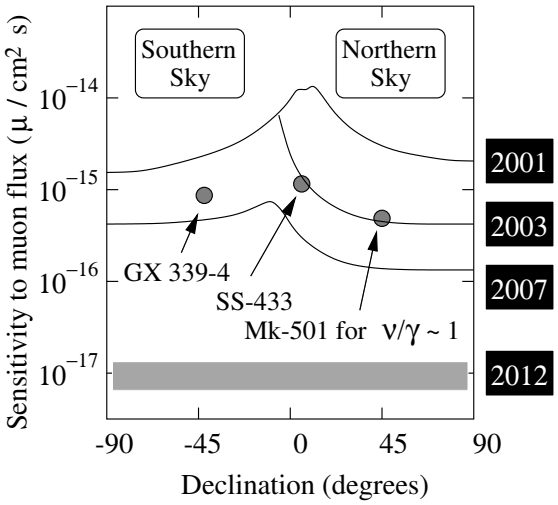

Figure 15. Scenario for the improvement of experimental sensitivities to TeV point sources. Expected steps for the Northern sky are obtained from Amanda (2003), and Amanda together with the first strings of IceCube (2007), on the Southern sky from the Mediterranean detectors Antares and Nestor (2007). In 2012, both hemispheres will have profited from cubic kilometer arrays indicated by the grey band. Shown are also predicted fluxes for two microquasars [46] - one on the northern and one on the southern hemisphere - which are just in reach for Amanda and the Mediterranean arrays. As a benchmark, we show also the flux which would be expected if Mk501, a source spectacular in TeV gamma rays, would produce a similar flux in TeV neutrinos.

Acknowledgment: I thank S. Barwick, P. Gorham, M. Kowalski and J. Learned for stimulating and helpful discussions. Furthermore, I acknowledge useful information and suggestions obtained from J. Brunner, A. Ringwald, D. Semikoz, A. Tsirigotis and Sh. Yoshida. This paper is a written version of talks given at the 18th European Cosmic Ray Conference, Moscow 2002, and the 8th Topical Seminar on Innovative Particle and Radiation Detectors, Siena 2002. I thank L. Kuzmichev and F. Navarria, respectively, for their kind invitations and their support.

REFERENCES

1. Neutrino Telescopes from lowest to highest energies are covered in J.G. Learned, Proc. 27th ICRC (2001), Invited, Review and Highlight papers, page 41.
2. J.G. Learned, K. Mannheim, Ann.Rev.Nucl. Phys. 50 (2000) 679.
3. see F. Halzen, astro-ph/0301143, for a recent comprehensive review of science goals as well as first results from Amanda.
4. K. Greisen, Phys.Rev.Lett. 16 (1966) 748; G.T. Zatsepin and V.A. Kuzmin, JETP.Lett 4 (1966) 78.
5. E. Waxman, J. Bahcall, Phys.Rev.D59 (1999) 023002.
6. V.S.Berezinsky and G.T.Zatsepin, Phys.Lett 28B (1969) 423.
7. K. Mannheim, R. Protheroe, J. Rachen, Phys. Rev.D63 (2001), 023003.
8. T.K. Gaisser, F. Halzen, T. Stanev, Phys. Rep.258 (1995) 173.
9. C. Spiering, Nucl. Phys. (Proc.Supp.) 91 (2000) 331 and astro-ph/0012532.
10. C. Spiering, Prog. in Part. and Nucl. Phys. 48 (2002) 43.
11. I.A.Belolaptikov et al., Astropart.Phys. 7 (1997) 263.
12. R.Balkanov et al., Astrop. Phys. 14 (2000) 61.
13. E. Andres et al., Astropart.Phys. 13 (2000) 1.
14. J. Ahrens et al., Limits on diffuse fluxes of high-energy extra-terrestrial neutrinos with the Amanda B10 detector, submitted to Phys. Lett.
15. J.Ahrens et al., Astrophys. J. 583 (2003) 1040, and astro-ph/0208006.
16. E. Andres et al., Nature 410 (2001) 441; J.Ahrens et al., Phys.Rev. D66 (2002) 012005.
17. see for recent results, Steve Barwick for the Amanda collaboration, astro-ph/0211269, and D. Cowen for the Amanda collaboration, astro-ph/0211264, and F.Halzen, ref.3.
18. A. Goldschmidt et al., Proc. 27th ICRC (2001) 1237 and C.Spiering et al., ibid. 1242.
19. T. Montaruli et al., hep-ex/0201009.
20. P. Grieder et al., Nucl.Phys. B (Proc.Suppl.) 97 (2001) 105.
21. T. Montaruli et al., hep-ex/9905019.
22. G. Askaryan, Sov.J.Atom.En. 3 (1957) 921.
23. L. Sulak et al., Nucl. Instr. Meth. 164 (1979) 267.
24. J.G. Learned, Phys.Rev. D1, 19 (1979) 3293.
25. P.B. Price, Astropart. Phys. 5 (1996) 43.
26. A. Capone et al., Proc. 27th ICRC (2001) 2164.
27. N. Lektinen et al., astro-ph/010433.
28. G.A. Askaryan, Sov. JETP 14 (1962) 441.
29. D. Saltzberg et al., Phys.Rev.Lett. 86 (2001) 2802.
30. D. Seckel et al., astro-ph/0103300.
31. P. Gorham et al., Nucl.Instr.Meth. A490 (2002) 476.
32. P. Gorham et al., JPL proposal A0-01-03-0SS-015 (2001).
33. P. Gorham et al., astro-ph/0102435.
34. A. Letessier-Selvon et al., Proc. 27th ICRC (2001) 1204.
35. M.Sasaki and M.Jobashi, astro-ph/0204167.
36. G.W.S.Hou, M.A.Huang, astro-ph/0204145.
37. R.Baltrusaitis et al., Phys.Rev. D31, 2192 (1985).
38. S. Yoshida et al., Proc. 27th ICRC (2001) 1142.
39. L. Scarsi et al., Proc.Int.Workshop on Neutrino Telescopes, Venice 2001, vol. II, 545.
40. D.B.Cline and F.W.Stecker, astro-ph/0003459.
41. H. Falcke and P. Gorham, astro-ph/0207226, subm. to Astropart. Physics.
42. see for a recent discussion of bounds and models O.Kalashev, V.Kuzmin, D.Semikoz and G.Sigl, Phys.Rev.D 66 (2002) 063004.
43. F.W.Stecker and M.H.Salomon, Space Sci. Rev. 75 (1996) 341.
44. G. Hill and M. Leuthold et al., Proc. 27th ICRC (2001) 1113.
45. the method is described in S. Hundertmark et al., Proc. 27th ICRC (2001) 1129.
46. C. DiStefano, D. Guetta, A. Levinson, E. Waxmann, ApJ 575 (2002) 378.